Efficient Electromagnetic Analysis of a Doubly Infinite Array of Rectangular Apertures

Andrew W. Mathis, *Student Member, IEEE,* and Andrew F. Peterson, *Senior Member, IEEE*

***Abstract*—An accurate and rapid method is presented for solving the magnetic field integral equation for the equivalent magnetic currents representing a doubly periodic array of rectangular apertures. Ewald's method is used to accelerate the summations associated with periodic Green's function, allowing the Green's function to be determined to nearly machine precision. Galerkin's method is used to discretize the integral equation with Chebyshev polynomials used as the basis and testing functions. Efficient treatment of the "self-term" singularity is emphasized.**

***Index Terms*—Diffraction gratings, electromagnetic scattering, frequency selective surfaces, moment methods.**

I. Introduction

THE SCATTERING from a periodically perforated conducting plane has important applications such as shielding, bandpass radomes, antenna reflectors, and ground planes for integrated circuits. Over the last few years, the accurate modeling of rectangular aperture arrays has also become increasingly important for thin-film multichip modules incorporating one or more perforated ground planes.

The methods used to solve the periodic aperture problem, as well as the complementary problem, scattering from a periodic array of plates, are various. Kieburtz and Ishimaru investigated the aperture problem employing a variational approach [1]. Chen solved both problems by discretizing the electric field or current density by orthogonal mode functions [2], [3]. Rubin and Bertoni used rooftop basis functions and razor-blade testing functions to solve for the current on the conductor surrounding arbitrarily shaped apertures [4]. This type of expansion is used in later work to analyze signal lines above a periodically perforated ground plane [5], [6]. Chan and Mittra refine this subsectional current approximation by using rooftop testing functions (Galerkin's method) [7], [8]. Pan, Zhu, and Gilbert approximate the equivalent magnetic current above the apertures in a periodically perforated ground plane [9]. In addition, they also use higher order basis functions to accelerate convergence of the doubly infinite summation in the periodic Green's function.

None of the methods above employ the exponentially converging form of the periodic Green's function developed by Jordon, Richter, and Sheng [10], which is based on Ewald's method [11]. For methods in [1]–[9], the convergence of the periodic Green's function is algebraic. At some point, the doubly infinite series of the Green's function is truncated, and with algebraic convergence it is difficult to determine the resulting truncation error. Ewald's method allows one to rapidly determine the value of the periodic Green's function to a prescribed accuracy (within a decimal place of machine precision) and eliminate truncation error as a major source of error. However, neither the original articles on Ewald's method, nor subsequent articles by Cohen [12], [13], describe a complete implementation and, in particular, how to handle the "self-term" in the integral equation formulation (where the source and observation regions coincide).

The purpose of this article is to present a complete implementation of the exponentially converging periodic Green's function for the problem involving an infinite periodic array of rectangular apertures in a ground plane. The approach presented herein employs the magnetic field integral equation and solves for the equivalent magnetic current within the apertures. Galerkin's method is used to discretize the integral equation with Chebyshev polynomials and their associated weights as the basis and testing functions. Entire domain functions which incorporate the edge singularity have been shown to require significantly fewer unknowns than subsectional basis functions or functions that do not incorporate the edge singularity [14], [15]. The use of entire domain basis functions implies that each element of the admittance matrix will require integration over a singularity when the source and observation regions coincide. To gain full advantage of Ewald's method, the singularity must be taken into account.

The geometry under consideration is depicted in Fig. 1. The apertures are rectangles of dimensions $2a \times 2b$. The center of the 00th aperture has the coordinate value $(x, y) = (0, 0)$. The entire structure exhibits periodicity D_x in the x-direction and D_y in the y-direction. A plane wave is incident upon the

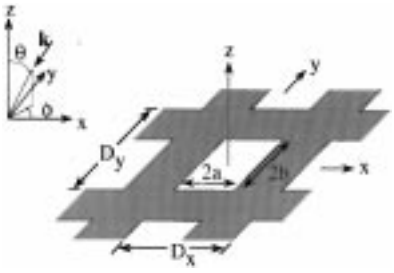

Fig. 1. A wave incident on a conducting plane periodically perforated with rectangular apertures.

Manuscript received October 29, 1996; revised October 9, 1997. This work was supported by the Packaging Research Center at Georgia Tech, which is funded under NSF EEC-9402723, ARPA, the State of Georgia, and a number of industrial partners.

The authors are with the Packaging Research Center, School of Electrical and Computer Engineering, Georgia Institute of Technology, Atlanta, GA 30332-0250 USA.

Publisher Item Identifier S 0018-9480(98)00630-9.

screen at an angle θ from the normal z-direction and at angle ϕ from the x-direction.

II. Formulation

The magnetic field integral equation for the equivalent magnetic current which is an infinitesimal distance above an aperture in a periodically perforated screen is

$$\boldsymbol{H}_{\tan} = j\frac{2}{k\eta}(k^2 + \nabla\nabla\cdot)\iint_S \boldsymbol{M}(\boldsymbol{r}')G_p(\boldsymbol{r},\boldsymbol{r}')\,d\mathcal{S}' \quad (1)$$

where $\mathcal{S}$ denotes a single aperture of the array, $\boldsymbol{M}$ is the equivalent magnetic current, $\boldsymbol{H}_{\tan}$ is the incident magnetic field produced in the aperture, and G_p is the three-dimensional (3-D) periodic Green's function.

The spectral domain form of the 3-D periodic Green's function, assuming $z = z'$, is

$$\begin{aligned} &G_p(x-x', y-y') \\ &\quad = \frac{1}{2D_xD_y}\sum_{p=-\infty}^{\infty}\sum_{q=-\infty}^{\infty} \\ &\qquad \cdot \frac{e^{jk_\xi(x-x')}e^{jk_\zeta(y-y')}}{jk_z}\bigg|_{\substack{k_\xi=(2\pi p/D_x)+k_x \\ k_\zeta=(2\pi q/D_y)+k_y}} \end{aligned} \quad (2)$$

where $jk_z = \sqrt{k_\xi^2 + k_\zeta^2 - k^2}$. Ewald's transformation of the 3-D periodic Green's function reduces to an error function transform (EFT) [16] when $z = z'$ and is written as [10]

$$G_p(x,y) = G_1(x,y) + G_2(x,y) \quad (3)$$

where

$$G_1(x,y) = \frac{1}{2D_xD_y}\sum_{p=-\infty}^{\infty}\sum_{q=-\infty}^{\infty}\frac{\operatorname{erfc}(jk_z/2E)}{jk_z}e^{jk_\xi x}e^{jk_\zeta y} \quad (4)$$

$$\begin{aligned} G_2(x,y) = &\frac{1}{8\pi}\sum_{p=-\infty}^{\infty}\sum_{q=-\infty}^{\infty}\frac{e^{-jk_xpD_x}e^{-jk_yqD_y}}{R_{pq}} \\ &\times\sum_{\pm}\left[e^{\pm jkR_{pq}}\operatorname{erfc}\left(R_{pq}E \pm j\frac{k}{2E}\right)\right] \end{aligned} \quad (5)$$

and

$$R_{pq} = \sqrt{(x-pD_x)^2 + (y-qD_y)^2} \quad (6)$$

where $\Sigma_\pm$ is the summation of the positive and the negative arguments. E is an arbitrarily chosen parameter that splits the computational burden between (4) and (5). The larger the value of E, the more weight (4) carries. Applying the Poisson sum transformation to (5) with respect to both p and q yields

$$G_2(x,y) = \frac{1}{2D_xD_y}\sum_{p=-\infty}^{\infty}\sum_{q=-\infty}^{\infty}\frac{\operatorname{erf}(jk_z/2E)}{jk_z}e^{jk_\xi x}e^{jk_\zeta y}. \quad (7)$$

Since $\operatorname{erfc} z + \operatorname{erf} z = 1$, adding (4) and (7) results in (2). Equations (4) and (5) are the EFT of the series in (2).

The magnetic-current components are assumed to have the form

$$M_x = \sqrt{\frac{1-(x/a)^2}{1-(y/b)^2}}\sum_{n=0}^{\infty}\sum_{m=0}^{\infty}M_x^{mn}U_n(x/a)T_m(y/b) \quad (8)$$

$$M_y = \sqrt{\frac{1-(y/b)^2}{1-(x/a)^2}}\sum_{n=0}^{\infty}\sum_{m=0}^{\infty}M_y^{mn}U_n(y/b)T_m(x/a) \quad (9)$$

where M^{mn} are unknown coefficients and T_n and U_n are nth-order Chebyshev polynomials of the first and second kind, respectively [17]. The equivalent magnetic current displays an inverse square-root singularity at the edges tangential to the direction of the current, and it must vanish at the edges normal to the direction of current. The Chebyshev functions satisfy both of the boundary conditions and are expected to converge rapidly to the solution. In a one-dimensional (1-D) case, three to four basis functions per wavelength are often deemed sufficient [18].

Using Galerkin's method to discretize the integral equation (1) yields a matrix equation with admittance elements of the form

$$Y_{i'i} = j\frac{2}{k\eta}(k^2 + \nabla\nabla\cdot)\boldsymbol{B}_{i'}(-x,-y) * \boldsymbol{B}_i(x,y) * G_p(x,y) \quad (10)$$

where

$$\boldsymbol{B}_i(x,y) = \begin{cases} \hat{\boldsymbol{x}}\sqrt{\dfrac{1-(x/a)^2}{1-(y/b)^2}}U_{n(i)}(x/a)T_{m(i)}(y/b), \\ \qquad\qquad \text{if } 1 \le i \le N_x \\ \hat{\boldsymbol{y}}\sqrt{\dfrac{1-(y/b)^2}{1-(x/a)^2}}U_{n(i)}(y/b)T_{m(i)}(x/a), \\ \qquad\qquad \text{if } N_x+1 \le i \le N_x+N_y \end{cases} \quad (11)$$

and * represents the two-dimensional (2-D) convolution operator. N_x and N_y represent the number of basis functions in the x- and y-directions, respectively. The spectral-domain representation of the Green's functions (4), (7) allows one to perform the convolutions in (10) analytically. With the help of (A.1) and (A.2), one obtains

$$\begin{aligned} Y_{A(i'i)} = &j\frac{2}{k\eta}\frac{\pi^4b^2j^{N_i}(n+1)(n'+1)(-1)^{n'+m'+1}}{2D_xD_y} \\ &\cdot\sum_{p=-\infty}^{\infty}\sum_{q=-\infty}^{\infty}\left(\frac{k^2}{k_\xi^2}-1\right) \\ &\times J_{n'+1}(k_\xi a)J_{n+1}(k_\xi a)J_{m'}(k_\zeta b)J_m(k_\zeta b) \\ &\cdot\left[\frac{\operatorname{erfc}(jk_z/2E)}{jk_z} + \frac{\operatorname{erf}(jk_z/2E)}{jk_z}\right] \end{aligned} \quad (12)$$

and

$$\begin{aligned} Y_{B(i'i)} = &-j\frac{2}{k\eta}\frac{\pi^4abj^{N_i}(m+1)(n'+1)(-1)^{n'+m'+1}}{2D_xD_y} \\ &\cdot\sum_{p=-\infty}^{\infty}\sum_{q=-\infty}^{\infty}J_{n'+1}(k_\xi a) \\ &\times J_n(k_\xi a)J_{m'}(k_\zeta b)J_{m+1}(k_\zeta b) \\ &\cdot\left[\frac{\operatorname{erfc}(jk_z/2E)}{jk_z} + \frac{\operatorname{erf}(jk_z/2E)}{jk_z}\right] \end{aligned} \quad (13)$$

where $N_i = n' + n + m' + m$, J_n is the nth-order Bessel function of the first kind, and the subscripts A and B denote a copolarization and a cross-polarization admittance term, respectively. Directional notation has been dropped since the admittance elements have the same form regardless of direction. The complementary error function appearing in both equations decays exponentially, and from (5), the error function displays a similar exponential convergence in the space domain. If the convolutions of (10) were performed using the space-domain Green's function of (5), the four-dimensional (4-D) numerical integration of a singular function is required. This method is numerically tedious if high accuracy is desired, especially if large apertures are under consideration. Consequently, a more efficient means of computing the space-domain part of the admittance element is sought.

III. Rapid Solution to the Integral Equation

The method employed here is to use Poisson's sum transformation of the error function terms of (12) and (13). Poisson's sum transformation is defined as

$$\sum_{p=-\infty}^{\infty} f(\alpha p) = \frac{1}{\alpha} \sum_{p=-\infty}^{\infty} F(2\pi p/\alpha) \tag{14}$$

where F is the Fourier transform of f. If the parameter E is chosen large enough, only the $p = 0$, $q = 0$ term is required to accurately approximate the space-domain part of the Green's function, (5). Due to the singularity associated with the "self-term," no value of E is large enough so that the space-domain part of the summation is negligible [16]. Since the aperture is centered at $(x, y) = (0, 0)$, the required inverse Fourier transforms reduce to

$$I_1 = \int_{-\infty}^{\infty}\int_{-\infty}^{\infty} J_{n_1}(k_\xi a) J_{n_2}(k_\xi a) J_{m_1}(k_\zeta b) \cdot J_{m_2}(k_\zeta b) \frac{\operatorname{erf}(jk_z/2E)}{jk_z}\, dk_\xi\, dk_\zeta \tag{15}$$

and

$$I_2 = \int_{-\infty}^{\infty}\int_{-\infty}^{\infty} \frac{J_{n_1}(k_\xi a) J_{n_2}(k_\xi a)}{k_\xi^2} \cdot J_{m_1}(k_\zeta b) J_{m_2}(k_\zeta b) \frac{\operatorname{erf}(jk_z/2E)}{jk_z} dk_\xi\, dk_\zeta. \tag{16}$$

The integral I_1 occurs in both copolarization admittance elements (12) and cross-polarization admittance elements (13), but the integral I_2 occurs only in the copolarization elements. Using the definition of the error function (A.21), (15) can be written as

$$I_1 = \frac{2}{\sqrt{\pi}} \int_0^{1/2E} e^{+k^2 s^2} \int_{-\infty}^{\infty} e^{-k_\xi^2 s^2} J_{n_1}(k_\xi a) J_{n_2}(k_\xi a)\, dk_\xi \times \int_{-\infty}^{\infty} e^{-k_\zeta^2 s^2} J_{m_1}(k_\zeta b) J_{m_2}(k_\zeta b)\, dk_\zeta\, ds. \tag{17}$$

If $n_1 + n_2$ or $m_1 + m_2$ is odd, then $I_1 = 0$. If not, the integral (A.3) is used to write (17) as

$$I_1 = \frac{a^N b^M}{2^{N+M}} \frac{\Gamma[(N+1)/2]\Gamma[(M+1)/2]}{n_1! n_2! m_1! m_2!} \frac{2}{\sqrt{\pi}} \cdot \int_0^{1/2E} \frac{e^{+k^2 s^2}}{s^{N+M+2}} {}_3F_3 \cdot \left(\frac{N+1}{2}, \frac{N+1}{2}, \frac{N}{2}+1;\ N+1; -\frac{a^2}{s^2}\right) \times {}_3F_3\left(\frac{M+1}{2}, \frac{M+1}{2}, \frac{M}{2}+1; m_1+1, m_2+1, M+1; -\frac{b^2}{s^2}\right) ds \tag{18}$$

where ${}_3F_3$ is a generalized hypergeometric function, $N = n_1 + n_2$ and $M = m_1 + m_2$. One notes the conditions of (A.3) are satisfied for $N, M \geq 0$. The generalized hypergeometric function is defined in (A.4). Following the same procedure, we can write (16) as

$$I_2 = \frac{a^N b^M}{2^{N+M}} \frac{\Gamma[(N-1)/2]\Gamma[(M+1)/2]}{n_1! n_2! m_1! m_2!} \frac{2}{\sqrt{\pi}} \int_0^{1/2E} \frac{e^{+k^2 s^2}}{s^{N+M}} \times {}_3F_3\left(\frac{N-1}{2}, \frac{N+1}{2}, \frac{N}{2}+1; n_1+1, n_2+1, N+1; -\frac{a^2}{s^2}\right) \times {}_3F_3\left(\frac{M+1}{2}, \frac{M+1}{2}, \frac{M}{2}+1; m_1+1, m_2+1, M+1; -\frac{b^2}{s^2}\right) ds. \tag{19}$$

For copolarization elements, the minimum values of N and M are two and zero, respectively. For $N \geq 2$ and $M \geq 0$, the conditions of (A.3) are satisfied. At first glance, the above integrals (18) and (19) appear to have strong singularities at $s = 0$, but these singularities are removable using the asymptotic expansion of the generalized hypergeometric function.

After substituting the asymptotic expansion derived in the Appendix for the hypergeometric function, we write (18) and (19) as

$$I_1 = \frac{1}{2^{N+M} ab} \frac{\Gamma[(N+1)/2]\Gamma[(M+1)/2]}{n_1! n_2! m_1! m_2!} \cdot \frac{2}{\sqrt{\pi}} \int_0^{1/2E} e^{+k^2 s^2} \sum_{i=0}^{N_A} (C_i^1 s^{2i} + D_i^1 s^{2i} \ln s + E_i^1 s^{2i} \ln^2 s)\, ds \tag{20}$$

$$I_2 = \frac{a/b}{2^{N+M}} \frac{\Gamma[(N-1)/2]\Gamma[(M+1)/2]}{n_1! n_2! m_1! m_2!} \cdot \frac{2}{\sqrt{\pi}} \int_0^{1/2E} e^{+k^2 s^2} \sum_{i=0}^{N_A} (C_i^2 s^{2i} + D_i^2 s^{2i} \ln s + E_i^2 s^{2i} \ln^2 s)\, ds \tag{21}$$

where N_A is the number of terms used in the asymptotic expansions. The coefficients C_i^λ, D_i^λ, and E_i^λ are defined as

$$C_i^\lambda = \sum_{l=0}^{i} \frac{A_l^{\lambda,n_1,n_2}}{a^{2l}} \frac{A_{(i-l)}^{1,m_1,m_2}}{b^{2(i-l)}} + D_{1,i}^\lambda \ln a + D_{2,i}^\lambda \ln b + E_i^\lambda \ln a \ln b \tag{22}$$

$$D_i^\lambda = -[D_{1,i}^\lambda + D_{2,i}^\lambda + E_i^\lambda(\ln a + \ln b)] \tag{23}$$

$$D_{1,i}^\lambda = 2\sum_{l=0}^{i} \frac{A_l^{\lambda,n_1,n_2}}{a^{2l}} \frac{B_{(i-l)}^{1,m_1,m_2}}{b^{2(i-l)}} \tag{24}$$

$$D_{2,i}^\lambda = 2\sum_{l=0}^{i} \frac{B_l^{\lambda,n_1,n_2}}{a^{2l}} \frac{A_{(i-l)}^{1,m_1,m_2}}{b^{2(i-l)}} \tag{25}$$

$$E_i^\lambda = 4\sum_{l=0}^{i} \frac{B_l^{\lambda,n_1,n_2}}{a^{2l}} \frac{B_{(i-l)}^{1,m_1,m_2}}{b^{2(i-l)}} \tag{26}$$

where A_l^{λ,n_1,n_2} and B_l^{λ,n_1,n_2} are the coefficients of the asymptotic approximation of the hypergeometric function that depend on the values of λ, n_1, and n_2. When $\lambda = 1$, the asymptotic approximation of ${}_3F_3$ (a_1, a_1, a_3; b_1, b_2, b_3; $-z$) is used, and when $\lambda = 2$, the asymptotic approximation of ${}_3F_3$ (a_1, a_1+1, a_3; b_1, b_2, b_3; $-z$) is used (see Appendix).

The value of E is assumed to be large; hence, the exponential term can be written as a power series as follows:

$$e^{+k^2 s^2} \simeq \sum_{i=0}^{N_A} \frac{k^{2i}}{i!} s^{2i}. \tag{27}$$

The power series (27) is multiplied with the power series in (22)–(26), and the result is integrated term-by-term. We can write the admittance elements as

$$Y_{A(i'i)} = -j\frac{2}{k\eta} \frac{\pi^4 b^2 j^{N+M} n_1 n_2 (-1)^{n_2+m_2}}{2D_x D_y} \cdot \left\{ \frac{D_x D_y}{4\pi^2}(I_2 - I_1) + \sum_{p=-P}^{P} \sum_{q=-Q}^{Q} \left(\frac{k^2}{k_\xi^2} - 1\right) \times J_{n_1}(k_\xi a) J_{n_2}(k_\xi a) J_{m_1}(k_\zeta b) J_{m_2}(k_\zeta b) \cdot \frac{\operatorname{erfc}(jk_z/2E)}{jk_z} \right\} \tag{28}$$

and

$$Y_{B(i'i)} = j\frac{2}{k\eta} \frac{\pi^4 ab j^{N+M} n_1 m_2 (-1)^{n_2+m_2}}{2D_x D_y} \cdot \left\{ \frac{D_x D_y}{4\pi^2} I_1 + \sum_{p=-P}^{P} \sum_{q=-Q}^{Q} J_{n_1}(k_\xi a) \times J_{n_2}(k_\zeta a) J_{m_1}(k_\zeta b) J_{m_2}(k_\zeta b) \frac{\operatorname{erfc}(jk_z/2E)}{jk_z} \right\} \tag{29}$$

where P and Q are the truncation values. I_1 and I_2 are functions of n_1, n_2, m_1, m_2, a, and b defined as

$$I_1 \approx \frac{2}{\sqrt{\pi}} \frac{1}{2^{N+M+1} ab} \frac{\Gamma[(N+1)/2]\Gamma[(M+1)/2]}{n_1! n_2! m_1! m_2!} \cdot \sum_{i=0}^{N_A} C_i' L_{2i}^0 + D_i' L_{2i}^1 + E_i' L_{2i}^2 \tag{30}$$

$$I_2 \approx \frac{2}{\sqrt{\pi}} \frac{a/b}{2^{N+M+1}} \frac{\Gamma[(N-1)/2]\Gamma[(M+1)/2]}{n_1! n_2! m_1! m_2!} \cdot \sum_{i=0}^{N_A} C_i' L_{2i}^0 + D_i' L_{2i}^1 + E_i' L_{2i}^2 \tag{31}$$

where C' is

$$C_i' = \sum_{l=0}^{i} \frac{k^{2l}}{l!} C_{i-l}. \tag{32}$$

The definitions of D' and E' are similar, and

$$L_i^l = \int_0^{1/2E} s^i (\ln s)^l \, ds \tag{33}$$

which is easily integrated analytically.

IV. The Parameter E

The choice of E directly relates to the convergence rate of the summations in (28) and (29). The parameter E needs to be chosen large enough so that only the 00th term is needed to accurately represent the space-domain part of the admittance element, yet E should be as small as possible so the spectral-domain part will converge rapidly. If one ignores the algebraic decay of (5), one finds that (5) decays as

$$\exp\left(-R_{pq}^2 E^2 + \frac{k^2}{4E^2}\right). \tag{34}$$

If the truncation error of the space-domain part is to be less than $\exp(-\psi^2)$, then

$$d^2 E^2 - \frac{k^2}{4E^2} \geq \psi^2 \tag{35}$$

where d is the minimum distance between apertures. If d is small, E must be large and can be approximated as

$$E \simeq \psi/d. \tag{36}$$

If d is not small

$$E = \sqrt{\frac{\psi^2}{d^2} + \frac{k^2}{4\psi^2}} \tag{37}$$

will satisfy (35). There are two other constraints on E: E needs to be chosen large enough so that the asymptotic approximation of the hypergeometric function and the power series expansion of (27) converge rapidly. If $E = 5/2\max(1/a, 1/b)$ then the asymptotic expansions usually converge to 15 significant figures within five to ten terms. If

TABLE I
CONVERGENCE OF COEFFICIENTS

N_x=N_y	2^2	4^2	6^2	8^2	10^2
M_x^{00}	316.981-j167.769	264.975-j15.6286	265.120-j13.6919	265.121-j13.6893	265.121-j13.6894
M_x^{02}	---	-210.941-j146.453	-206.693-j149.910	-206.691-j149.930	-206.688-j149.932
M_x^{20}	---	-46.219+j94.480	-46.519+j98.225	-46.509+j98.234	-46.505+j98.238
M_x^{22}	---	28.594-j15.511	27.730-j15.680	27.744-j15.699	27.748-j15.696
τ	0.31898	0.28832	0.28790	0.28790	0.28790
Rel. Time	1.0	7.5	31.5	111	271

$E \geq k/2$, the power series of (27) will converge rapidly over the entire range of integration. To summarize, E is typically chosen as

$$E \geq \max\{\psi/d, 5/2\max(1/a, 1/b), k/2\}. \tag{38}$$

For small apertures $(a,b<1\lambda)$, the first condition dominates, for medium apertures $(1\lambda \leq a,b, <3\lambda)$, the second condition dominates, and for large apertures $(a,b>3\lambda)$, the third condition dominates. To determine where to truncate the summation, we ignore the algebraic decay of the spectral-domain summation and only use the exponential decay from complementary error function. The truncation values $P \geq E\psi D_x/\pi$ and $Q \geq E\psi D_y/\pi$ are appropriate.

V. RESULTS

Although the implementation of the spectral-domain part of the admittance element is straightforward, the majority of the computational effort goes to evaluating the summations in (28) and (29). This is due to the four Bessel functions and the complementary error function that must be computed. If the argument of the complementary error functions is imaginary, the algorithm of [19] and [20], which is a refined version of [21] and [22], can be used. If the argument is real, then a Chebyshev approximation can be used [23]. The Bessel functions are computed using routines from NETLIB[1] written by Cody. Efficient evaluation of I_1 and I_2 relies on rapidly computing the values of the coefficients of the asymptotic expansion of the generalized hypergeometric functions. Typically $N_A = 5$ is sufficient for seven significant figures of accuracy and $N_A = 10$ is sufficient for 15 significant figures of accuracy. All calculations were performed in double precision (16 significant figures).

Consider a conducting plane with $1.0\lambda \times 1.0\lambda$ apertures and a periodicity of $D_x = D_y = 1.75\lambda$ excited by an incident plane wave $\boldsymbol{H} = \hat{\boldsymbol{x}}e^{-jkz}$. For this case, $E = 10.7$ ensures that each admittance element has converged to 15 significant figures. Typically less accuracy is required, and E can be decreased. In Fig. 2, the relative error of a copolarization admittance element truncated at $P = Q$ is shown for differing values of the parameter E. The admittance element corresponds to $n' = n = m' = m = 0$. The Y_{exact} is determined by setting $E = 30$ and $P = Q = 84$. As is expected, the summation converges slower as E increases, but exponential convergence is observed for all finite E. When $E \to \infty$, the admittance element reverts completely to the spectral domain and converges at the rate $O[(pq)^{-1}(p^2+q^2)^{-1/2}]$ as $p,q \to \infty$.

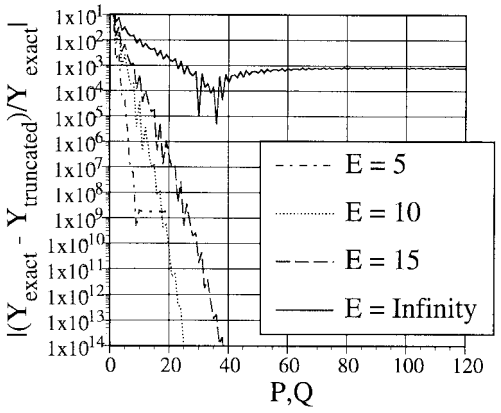

Fig. 2. The relative error of the admittance element corresponding to $n' = n = m' = m = 0$ truncated at $P = Q$.

In Fig. 3, the real and imaginary parts of the equivalent magnetic current in the x-direction normalized with respect to the incident electric field are shown. For Fig. 3, the number of basis functions is $N_x = N_y = 6^2$. This implies that the coefficients of interest are M_x^{nm}, M_y^{nm} for $0 \leq n,m<(6-1)$. The superscripts n and m correspond to the order of the Chebyshev polynomials as described in (8) and (9). The choices $E = 10.7$ and $P = Q = 25$ ensure 15 digits of accuracy. Thus, the discretization error inherent in Galerkin's method is the only significant source of error, i.e., truncation error is negligible. In Fig. 4, the magnitude of the normalized magnetic current in the x-direction along a line $(y = 0)$ tangential to the current is plotted for various basis sets $N_x = N_y = N^2$. As expected, the solution rapidly converges.

In Table I, the values of the coefficients M_x^{00}, M_x^{02}, M_x^{20}, and M_x^{22} are shown for differing $N_x = N_y = N^2$. These coefficients are the dominant coefficients that appear in all the basis sets for $N_x = N_y \geq 4^2$. The power transmission

[1] Available at http://www.netlib.org/.

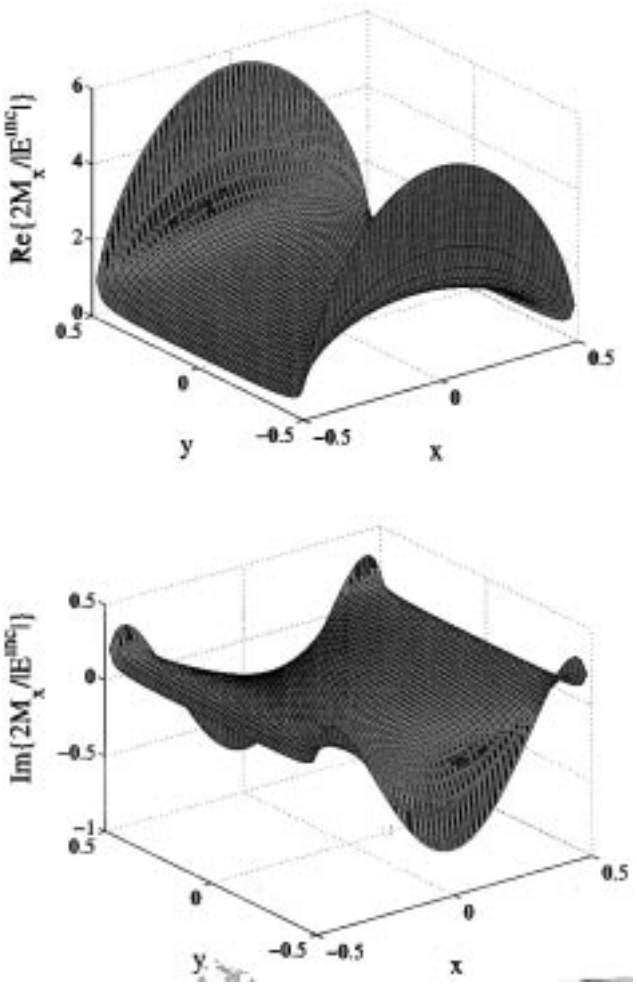

Fig. 3. The real and imaginary part of the x-directed magnetic current normalized with respect to the incident electric field $E = \hat{y}\eta e^{-jkz}$. The aperture dimensions are $a = b = 0.5\lambda$ and the periodicity is $D_x = D_y = 1.75\lambda$.

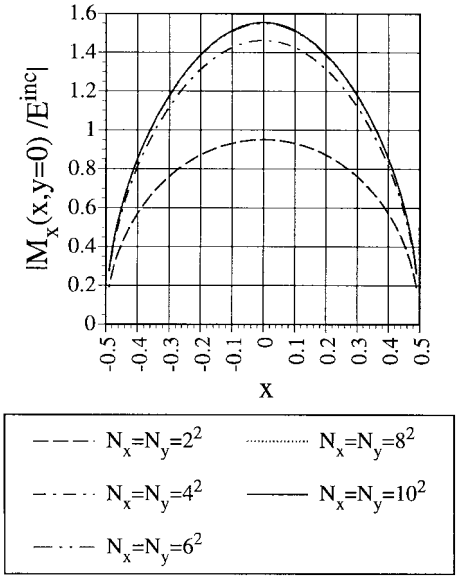

Fig. 4. The magnitude of the normalized magnetic current in the x-direction along a line $(y = 0)$ tangential to the current for various sets of basis functions. The geometry of the problem is identical to that of Fig. 3.

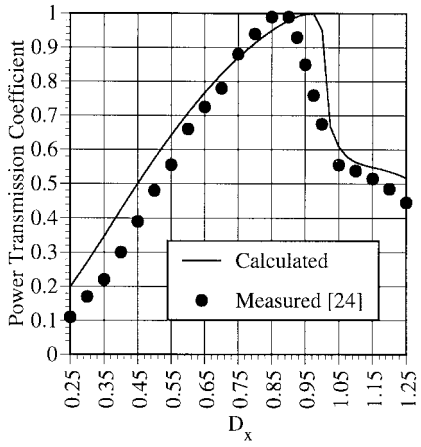

Fig. 5. The magnitude of the power transmission coefficient versus periodicity D_x. The aperture dimensions are $a = b = 0.39D_x$, and the incident magnetic field is $\boldsymbol{H} = \hat{x}e^{-jkz}$.

coefficient τ is shown for the various basis sets, and the transmission converges to five digits of accuracy for $N_x = N_y = 6^2$. The relative time required to solve the integral equation for the various sets of basis functions is also shown. This time includes both the matrix fill and matrix solve time and is normalized with respect to the time required for the $N_x = N_y = 2^2$ case. It should be noted that the value $E = 10.7$ overly restricts the efficiency for this example. If E is dropped to 5.4 (ensuring eight significant figures of accuracy in the admittance elements), then $P = Q = 7$ and the time required for the $N_x = N_y = 6^2$ case is reduced by 87% with no significant change in the dominant coefficients.

In Fig. 5, the power transmission coefficient versus periodicity is presented. The magnetic field $\boldsymbol{H} = \hat{\boldsymbol{x}}e^{-jkz}$ is incident on an array of square apertures $(a = b)$ with a periodicity of $D_x = D_y$. The ratio of aperture size to periodicity is held at $a = 0.39D_x$. The power transmitted is compared to the measured data from [24]. Good agreement is obtained between the two.

VI. Conclusion

A method is presented for rapidly and accurately solving the magnetic field integral equation for doubly periodic array of rectangular apertures. The technique is based on Ewald's method for accelerating the periodic Green's function, which if used correctly, reduces the truncation error so that it is negligible compared to the discretization error. This method works very well for small-to-medium size apertures. As the aperture size increases, E also increases, making the spectral-domain summation more expensive.

Although this technique is discussed in the context of rectangular apertures, it can be generalized to other aperture shapes. The integral (A.3) is derived by converting the product of two Bessel functions into the hypergeometric function ${}_2F_3$. The integral from zero to infinity of the hypergeometric function ${}_nF_m$ multiplied by a Gaussian function is the hypergeometric function ${}_{(n+1)}F_m$ [27]. Thus, the technique can be generalized when the spectral-domain representation of the basis and testing functions can be expressed in terms of a hypergeometric

function and the basis and testing functions are centered about the same point ($x = x'$, $y = y'$, and $z = z'$).

MATHEMATICAL APPENDIX

This appendix summarizes several results used in the previous sections.

A. Useful Integrals

The Fourier transforms of the Chebyshev basis functions are given by the following integrals [17]:

$$\int_{-w}^{w} \frac{T_n(x/w)e^{j\zeta x}}{\sqrt{1-(x/w)^2}}\,dx = \pi w j^n J_n(w\zeta) \quad \text{(A.1)}$$

$$\int_{-w}^{w} \sqrt{1-(x/w)^2}U_n(x/w)e^{j\zeta x}\,dx = \pi j^n \frac{n+1}{\zeta} J_{n+1}(w\zeta). \quad \text{(A.2)}$$

The following integral is used in determining the space-domain contribution of the 00th plate [see (17) and (18)] [25]:

$$\int_0^\infty x^{\lambda-1}e^{-\alpha^2x^2}J_\nu(\beta x)J_\mu(\beta x)\,dx = \frac{(\beta/2)^{\mu+\nu}}{2\alpha^{\nu+\mu+\lambda}}\frac{\Gamma[(\mu+\nu+\lambda)/2]}{\Gamma(\nu+1)\Gamma(\mu+1)} \times {}_3F_3\left[\frac{\nu+\mu+1}{2}, \frac{\nu+\mu}{2}+1, \frac{\nu+\mu+\lambda}{2}; \nu+1, \mu+1, \nu+\mu+1; -\frac{\beta^2}{\alpha^2}\right] \quad \text{(A.3)}$$

where $\mathrm{Re}(\lambda+\mu+\nu) > 0$ and $\mathrm{Re}(\alpha^2) > 0$.

B. Asymptotic Approximation of ${}_3F_3\,(a_1, a_2, a_3; b_1, b_2, b_3; -z)$

Methods are readily available for determining the asymptotic approximation of generalized hypergeometic functions if a_1, a_2, a_3 do not differ by an integer [26], [27]. From (18) and (19), $a_1 - a_2$ will equal zero or one; hence, we need to derive an asymptotic approximation that is valid for $a_1 - a_2$ equal to an integer. The function ${}_3F_3\,(a_1, a_2, a_3; b_1, b_2, b_3; -z)$ is defined as

$${}_3F_3(a_1,a_2,a_3;b_1,b_2,b_3;-z) = \frac{\Gamma(b_1)\Gamma(b_2)\Gamma(b_3)}{\Gamma(a_1)\Gamma(a_2)\Gamma(a_3)}\sum_{n=0}^{\infty}\frac{\Gamma(a_1+n)\Gamma(a_2+n)}{\Gamma(b_1+n)\Gamma(b_2+n)} \times \frac{\Gamma(a_3+n)}{\Gamma(b_3+n)}\frac{(-z)^n}{n!} \quad \text{(A.4)}$$

where Γ is the Gamma function. We can write the above series in terms of the following inverse Mellin transform:

$${}_3F_3(a_1,a_2,a_3;b_1,b_2,b_3;-z) = \frac{1}{2\pi}\frac{\Gamma(b_1)\Gamma(b_2)\Gamma(b_3)}{\Gamma(a_1)\Gamma(a_2)\Gamma(a_3)}\int_{\gamma-i\infty}^{\gamma+i\infty}\frac{\Gamma(a_1-s)\Gamma(a_2-s)}{\Gamma(b_1-s)\Gamma(b_2-s)} \times \frac{\Gamma(a_3-s)\Gamma(s)}{\Gamma(b_3-s)}z^{-s}\,ds. \quad \text{(A.5)}$$

Extending the path of integration counterclockwise to make a semicircle with a radius of infinity, one finds the value of the integral equals the sum of the residues ($\times 2\pi$) of the simple poles from the $\Gamma(s)$ term. Thus, one regains (A.4). Equation (A.5) is equivalent to using the definition of the Meijer G function to express the hypergeometric function [25]–[27].

To obtain an asymptotic approximation of ${}_3F_3\,(a_1, a_2, a_3; b_1, b_2, b_3; -z)$, we extend the path of integration clockwise to form a semicircle encompassing the positive real values for s. If a_1 and a_2 do not differ by an integer then the integral is evaluated by summing the residues from the simple poles at $s = a_1 + n$, $a_2 + n$, $a_3 + n$. If $a_1 - a_2$ does equal an integer, some or all of the poles will be double poles and one must differentiate the nonsingular part of the integrand of (A.5) to determine the residue. There are two cases of interest $a_1 = a_2$ and $a_1 = a_2 - 1$. For the case $a_1 = a_2$, the residues are

$$\operatorname*{Res}_{s\to a_1+n}\frac{\Gamma^2(a_1-s)\Gamma(a_3-s)\Gamma(s)}{\Gamma(b_1-s)\Gamma(b_2-s)\Gamma(b_3-s)}z^{-s} = R_n^2 z^{-(a_1+n)}(R_n^1 - \ln\, z) \quad \text{(A.6)}$$

where

$$R_n^1 = -2\Psi(n) + \Psi(a_1+n) - \Psi(a_3-a_1-n) + \sum_{i=1}^{3}\Psi(b_i-a_1-n) \quad \text{(A.7)}$$

$$R_n^2 = \frac{\Gamma(a_1+n)\Gamma(a_3-a_1-n)}{(n!)^2\prod_{i=1}^{3}\Gamma(b_i-a_1-n)} \quad \text{(A.8)}$$

and Ψ is the digamma function. For the case $a_1 = a_2 - 1$, the residues from the double poles are

$$\operatorname*{Res}_{s\to a_1+n}\frac{\Gamma(a_1-s)\Gamma(a_1+1-s)\Gamma(a_3-s)\Gamma(s)}{\Gamma(b_1-s)\Gamma(b_2-s)\Gamma(b_3-s)}z^{-s} = R_n^2 z^{-(a_1+n)}(R_n^1 - \ln\, z) \quad \text{(A.9)}$$

where

$$R_n^1 = \Psi(n+1) + \Psi(n) - \Psi(a_1+n) + \Psi(a_3-a_1-n) - \sum_{i=1}^{3}\Psi(b_i-a_1-n) \quad \text{(A.10)}$$

$$R_n^2 = \frac{\Gamma(a_1+n)\Gamma(a_3-a_1-n)}{n!(n-1)!\prod_{i=1}^{3}\Gamma(b_i-a_1-n)}. \quad \text{(A.11)}$$

The residue from the single pole at $s = a_1$ is $R_0^2 z^{-a_1}$. For both cases, the residues from the single poles at $s = a_3 + n$ equal

$$\operatorname*{Res}_{s\to a_3+n}\frac{\Gamma(a_1-s)\Gamma(a_2-s)\Gamma(a_3-s)\Gamma(s)}{\Gamma(b_1-s)\Gamma(b_2-s)\Gamma(b_3-s)}z^{-s} = R_n^3 z^{-(a_3+n)} \quad \text{(A.12)}$$

where

$$R_n^3 = \frac{\Gamma(a_1-a_3-n)\Gamma(a_2-a_3-n)\Gamma(a_3+n)}{n!\prod_{i=1}^{3}\Gamma(b_i-a_1-n)}. \quad \text{(A.13)}$$

Using the values of the residues, the asymptotic approximation for hypergeometric function in (18) is

$$ {}_3F_3(a_1,a_1,a_3;b_1,b_2,b_3;-z) = \sum_i A_i z^{-(a_1+i)} + B_i z^{-(a_1+i)} \ln z + C_i z^{-(a_3+i)} \quad \text{(A.14)} $$

where for general arguments (a_1, a_2, a_3, b_1, b_2, b_3):

$$ A_i = -\frac{\Gamma(b_1)\Gamma(b_2)\Gamma(b_3)}{\Gamma(a_1)\Gamma(a_2)\Gamma(a_3)} R_n^1 R_n^2 \quad \text{(A.15)} $$

$$ B_i = -\frac{\Gamma(b_1)\Gamma(b_2)\Gamma(b_3)}{\Gamma(a_1)\Gamma(a_2)\Gamma(a_3)} R_n^2 \quad \text{(A.16)} $$

$$ C_i = -\frac{\Gamma(b_1)\Gamma(b_2)\Gamma(b_3)}{\Gamma(a_1)\Gamma(a_2)\Gamma(a_3)} R_n^3. \quad \text{(A.17)} $$

The hypergeometric function in (19) has the asymptotic expansion

$$ {}_3F_3(a_1,a_1+1,a_3;b_1,b_2,b_3;-z) = \sum_i A_i z^{-(a_1+i)} + B_i z^{-(a_1+1+i)} \ln z + C_i z^{-(a_3+i)} \quad \text{(A.18)} $$

where A, B, and C are defined similar to (A.15)–(A.17), except $A_0 = R_0^2$. For the values of the arguments a_3, b_1, b_2, b_3 under consideration in (18) and (19), $R_n^3 = 0$ and, consequently, $C_i = 0$. This is because a_3, b_1, b_2, and b_3 differ by integers and $a_3 \leq b_1, b_2$; hence, either $\Gamma(b_1 - a_3)$ or $\Gamma(b_2 - a_3)$ will equal infinity. This means that all ${}_3F_3$ functions generated in (18) and (19) are reducible to ${}_2F_2$ or combinations of ${}_2F_2$. For example, if $n_1 = n_2$ then $N/2+1 = n_1+1 = n_2+1$; hence

$$ {}_3F_3\left(\frac{N\pm1}{2}, \frac{N+1}{2}, \frac{N}{2}+1; n_1+1, n_2+1, N+1; -z^2\right) = {}_2F_2\left(\frac{N\pm1}{2}, \frac{N+1}{2}; n_2+1, N+1; -z^2\right). \quad \text{(A.19)} $$

If $n_1 = 2$ and $n_2 = 0$ (or vice-versa) in (18), we obtain

$$ {}_3F_3\left(\frac{3}{2}, \frac{3}{2}, 2; 1, 3, 3; -z^2\right) = {}_2F_2\left(\frac{3}{2}, \frac{3}{2}; 3, 3; -z^2\right) - \left(\frac{z^2}{4}\right) {}_2F_2\left(\frac{5}{2}, \frac{5}{2}; 4, 4; -z^2\right). \quad \text{(A.20)} $$

Further details on obtaining an asymptotic expansion from a power series can be found in [28]. It should be noted that the above asymptotic approximation is only valid for large positive values of z. Due to the essential singularity at $z = -\infty$, (A.4) cannot be used to obtain an asymptotic approximation valid for $z < 0$. For large negative values for z where higher order terms dominate the summation of (A.4), the hypergeometric function increases exponentially with $-z$.

C. The Error Function

The error function and the complementary error function are defined, respectively, as

$$ \operatorname{erf} z = \frac{2}{\sqrt{\pi}} \int_0^z e^{-u^2}\, du \quad \text{(A.21)} $$

$$ \operatorname{erfc} z = 1 - \operatorname{erf} z = \frac{2}{\sqrt{\pi}} \int_z^\infty e^{-u^2}\, du. \quad \text{(A.22)} $$

As $z \to \infty$, the complementary error function behaves as

$$ \operatorname{erfc} z \sim \frac{e^{-z^2}}{\sqrt{\pi} z}. \quad \text{(A.23)} $$

REFERENCES

[1] R. B. Kieburtz and A. Ishimaru, "Aperture fields of an array of rectangular apertures," *IEEE Trans. Antennas Propagat.*, vol. AP-9, pp. 506–514, Nov. 1961.

[2] C. C. Chen, "Transmission through a conducting screen perforated periodically with apertures," *IEEE Trans. Microwave Theory Tech.*, vol. MTT-18, pp. 627–632, Sept. 1970.

[3] ——, "Scattering by a two-dimensional periodic array of conducting plates," *IEEE Trans. Antenna Propagat.*, vol. AP-18, pp. 660–665, Sept. 1970.

[4] B. Rubin and H. Bertoni, "Reflection from a periodically perforated plane using a subsectional current approximation," *IEEE Trans. Antennas Propagat.*, vol. AP-31, pp. 829–836, Nov. 1983.

[5] ——, "Waves guided by conductive strips above a periodical perforated ground plane," *IEEE Trans. Microwave Theory Tech.*, vol. MTT-31, pp. 541–549, July 1983.

[6] B. Rubin, "The propagation characteristics of signal lines in a mesh plane environment," *IEEE Trans. Microwave Theory Tech.*, vol. MTT-32, pp. 522–531, May 1984.

[7] C. H. Chan and R. Mittra, "On the analysis of frequency selective surfaces using subdomain basis functions," *IEEE Trans. Antennas Propagat.*, vol. 38, pp. 40–50, Jan. 1990.

[8] ——, "The propagation characteristics of signal lines embedded in a multilayered structure in the presence of periodically perforated ground plane," *IEEE Trans. Microwave Theory Tech.*, vol. 36, pp. 968–975, June 1988.

[9] G. Pan, X. Zhu, and B. Gilbert, "Analysis of transmission lines of finite thickness above a periodically perforated ground plane at oblique orientations," *IEEE Trans. Microwave Theory Tech.*, vol. 43, pp. 383–392, Feb. 1995.

[10] K. E. Jordan, G. R. Richter, and P. Sheng, "An efficient numerical evaluation of the Green's function for the Helmholtz operator on periodic structures," *J. Comp. Phys.*, vol. 43, pp. 222–235, 1986.

[11] P. P. Ewald, "Die berechnung optischer und elektrostatischen gitterpotentiale," *Ann. Phys.*, (Germany), vol. 64, pp. 253–268, 1921.

[12] E. Cohen, "Critical distance for grating lobe series," *IEEE Trans. Antennas Propagat.*, vol. 39, pp. 677–679, May 1991.

[13] ——, "An Ewald transformation of frequency domain integral formulations," *Electromagnetics*, vol. 15, pp. 427–439, 1995.

[14] W. C. Chew and Q. Liu, "Resonance frequency of a rectangular microstrip patch," *IEEE Trans. Antennas Propagat.*, vol. 36, pp. 1045–1056, Aug. 1988.

[15] D. I. Kaklamani and N. K. Uzunoglu, "Scattering from a conductive rectangular plate covered by a thick dielectric layer excited by a dipole source or a plane wave," *IEEE Trans. Antennas Propagat.*, vol. 42, pp. 1065–1076, Aug. 1994.

[16] A. W. Mathis and A. F. Peterson, "A comparison of acceleration procedures for the two-dimensional periodic Green's function," *IEEE Trans. Antennas Propagat.*, vol. 44, pp. 567–571, Apr. 1996.

[17] M. Abramowitz and I. Stegun, Eds., *Handbook of Mathematical Functions.* New York: Dover, 1972.

[18] D. Gottlieb, M. Y. Hussaini, and S. A. Orszag, "Introduction: Theory and applications of spectral methods," in *Spectral Methods for Partial Differential Equations*, R. G. Voight, D. Gottlieb, and M. Yousuff Hussaini, Eds. Philadelphia: SIAM, 1984, pp. 1–54..

[19] G. P. M. Poppe and C. M. J. Wijers, "More efficient computation of the complex error function," *ACM Trans. Math. Softw.*, vol. 16, pp. 38–46, 1990.

[20] G. P. M. Poppe and C. M. J. Wijers, "Algorithm 680—More efficient computation of the complex error function," *ACM Trans. Math. Softw.*, vol. 16, p. 47, 1990.

[21] W. Gautschi, "Efficient computation of the complex error function," *ACM Trans. Math. Softw.*, vol. 7, no. 1, pp. 187–198, Mar. 1970.
[22] W. Gautschi, "Algorithm 363, complex error function," *Commun. ACM*, vol. 12, no. 11, p. 635, Nov. 1969.
[23] W. J. Cody, "Rational Chebyshev approximations for the error function," *Math. Comput.*, vol. 8, pp. 631–638, 1969.
[24] R. Ulrich, "Far-IR optical properties of freestanding and dielectrically backed metal meshes," *Appl. Opt.*, vol. 20, no. 7, pp. 1245–1253, Apr. 1981.
[25] I. S. Gradshteyn and I. M. Ryzhik, *Table of Integrals, Series, and Products.* New York: Academic, 1980.
[26] L. J. Slater, *Generalized Hypergeometric Functions.* Cambridge, U.K.: Cambridge Univ. Press, 1966.
[27] A. M. Mathai, *Generalized Hypergeometric Functions with Applications in Statistics and Physical Sciences.* Berlin, Germany: Springer-Verlag, 1973.
[28] R. B. Dingle, *Asymptotic Expansions: Their Derivation and Interpretation.* New York: Academic, 1973.

Andrew W. Mathis (S'94) was born in Miami, FL, in 1969. He received the B.S. and M.S. degrees in electrical engineering from Clemson University, Clemson, SC, in 1991 and 1993, respectively, and is currently working toward the Ph.D. degree in electrical engineering at Georgia Institute of Technology, Atlanta.

From 1991 to 1993, he was employed as a Teaching Assistant and Research Assistant at Clemson University. In 1994, he joined the Packaging Research Center, Georgia Institute of Technology. His current research interests include computational methods in electromagnetic and electromagnetic aspects of electronic packaging including via analysis and interconnect modeling.

Andrew F. Peterson (S'82–M'83–SM'92) received the B.S., M.S., and Ph.D. degrees in electrical engineering from the University of Illinois at Urbana-Champaign, in 1982, 1983, and 1986, respectively.

Since 1989, he has been a Faculty Member of the School of Electrical and Computer Engineering, Georgia Institute of Technology, Atlanta, where he is currently an Associate Professor teaching electromagnetic-field theory and computational electromagnetics, and conducting research in the development of computational techniques for electromagnetic scattering, microwave devices, and electronic packaging applications.

Dr. Peterson is a member of URSI Commission B, ASEE, and AAUP. He has served as an associate editor of the IEEE TRANSACTIONS ON ANTENNAS AND PROPAGATION, chairman of the Atlanta joint IEEE AP-S/MTT chapter, and is currently the general chair of the 1998 IEEE AP-S International Symposium and URSI National Radio Science Meeting, Atlanta, GA. He has also served for six years as a director of ACES.